

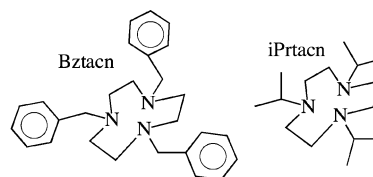
A Tetranuclear $\text{Cr}^{\text{III}}\text{Ni}^{\text{II}}_3$ Cyano-Bridged Complex Based on M(tacn) Derivative Building Blocks

Jean-Noël Rebilly,[†] Laure Catala,[†] Eric Rivière,[†] Régis Guillot,[†] Wolfgang Wernsdorfer,[‡] and Talal Mallah^{*,†}

Laboratoire de Chimie Inorganique, ICMO, CNRS UMR 8613, Université Paris-Sud, 91405 Orsay, France, and Laboratoire Louis Néel, CNRS, 25 Avenue des Martyrs, BP166, 38042 Grenoble, Cedex 9, France

Received August 24, 2005

The reaction of $\text{Cr}(\text{Bztacn})(\text{CN})_3$ (Bztacn is 1,4,7-trisbenzyl-1,4,7-triazacyclononane) with $\text{Ni}(\text{iPrtacn})\text{Cl}_2$ (iPrtacn is 1,4,7-tris(isopropyl)-1,4,7-triazacyclononane) affords a CrNi_3 tetranuclear complex. Variable temperature and magnetization versus field measurements show a $S = 9/2$ ground state and an appreciable magnetic anisotropy with a negative $D_{9/2}$ value equal to -0.54 cm^{-1} . Magnetization studies on one single crystal using a micro-SQUID show a fast tunneling process at zero field at very low temperature.



$\text{BztacnCr}(\text{CN})_3$ and $\text{Ni}(\text{iPrtacn})\text{Cl}_2$ in methanol (Bztacn is 1,4,7-trisbenzyl-1,4,7-triazacyclononane and iPrtacn is 1,4,7-tris(isopropyl)-1,4,7-triazacyclononane).^{4,5} Because the $\text{BztacnCr}(\text{CN})_3$ complex is almost insoluble in common solvents,⁴ it was added as a solid to the Ni-containing solution. A color change (yellow to green) followed by a complete dissolution of the chromium complex occurred. Green needlelike single crystals suitable for structure determination grew within a

Since the report of the first polynuclear high-spin complexes using cyanides as the bridging ligand to transmit the electronic information between the paramagnetic ions,¹ much effort has been invested to prepare new complexes mainly using a stepwise approach.² New bimetallic complexes including some showing single-molecule magnet behavior have been discovered during the past few years.³ Recently, using a two-step synthetic approach, Dunbar and co-workers obtained a trimetallic complex thanks to the presence of the chemically inert $\text{Co}(\text{III})$ ions.^{2s,t}

In this Communication, we report the preparation, the crystal structure, and the magnetic behavior of a tetranuclear $\text{Cr}^{\text{III}}\text{Ni}^{\text{II}}_3$ complex using triazacyclononane derivatives as blocking ligands. Triazacyclononane-based complexes had first been successfully used by Long and co-workers, and a variety of complexes with different architectures were stabilized.^{2r}

The tetranuclear complex of formula $[\text{BztacnCr}(\text{CNNi}(\text{iPrtacn})\text{Cl})_3]\text{Cl}_3 \cdot 10\text{H}_2\text{O}$ (**1**; see scheme for Bztacn and iPrtacn) was obtained from the stoichiometric reaction of

- (2) (a) Heinrich, J. L.; Berseth, P. A.; Long, J. R. *Chem. Commun.* **1998**, 1231. (b) Marvilliers, A.; Pei, Y.; Cano Boquera, J.; Vostrikova, K. E.; Paulsen, C.; Rivière, E.; Audié, J.-P.; Mallah, T. *Chem. Commun.* **1999**, 1951. (c) Vostrikova, K. E.; Luneau, D.; Wernsdorfer, W.; Rey, P.; Verdager, M. *J. Am. Chem. Soc.* **2000**, *122*, 718. (d) Berseth, P. A.; Sokol, J. J.; Shores, M. P.; Heinrich, J. L.; Long, J. R. *J. Am. Chem. Soc.* **2000**, *122*, 9655. (e) Sokol, J. J.; Shores, M. P.; Long, J. R. *Angew. Chem., Int. Ed.* **2001**, *40*, 236. (f) Heinrich, J. L.; Sokol, J. J.; Hee, A. G.; Long, J. R. *J. Solid State Chem.* **2001**, *159*, 293. (g) Smith, J. A.; Galan-Mascaros, J. R.; Clérac, R.; Sun, J. S.; Xiang, O. Y.; Dunbar, K. R. *Polyhedron* **2001**, *20*, 1727. (h) Rogez, G.; Parsons, S.; Paulsen, C.; Villar, V.; Mallah, T. *Inorg. Chem.* **2001**, *40*, 3836. (i) Sokol, J. J.; Shores, M. P.; Long, J. R. *Inorg. Chem.* **2002**, *41*, 3052. (j) Lescouëzec, R.; Vaissermann, J.; Lloret, F.; Julve, M.; Verdager, M. *Inorg. Chem.* **2002**, *41*, 5943. (k) Podgajny, R.; Desplanches, C.; Sieklucka, B.; Sessoli, R.; Villar, V.; Paulsen, C.; Wernsdorfer, W.; Dromzee, Y.; Verdager, M. *Inorg. Chem.* **2002**, *41*, 1323. (l) Rogez, G.; Marvilliers, A.; Sarr, P.; Parsons, S.; Teat, S. J.; Ricard, L.; Mallah, T. *Chem. Commun.* **2002**, 1460. (m) Si, S. F.; Tang, J. K.; Liu Liao, D. Z.; Jiang, Z. H.; Yan, S. P.; Cheng, P. *Inorg. Chem. Commun.* **2003**, *6*, 1109. (n) Marvaud, V.; Decroix, C.; Scullier, A.; Guyard-Duhayon, C.; Vaissermann, J.; Gonnet, F.; Verdager, M. *Chem. Eur. J.* **2003**, *9*, 1678. (o) Wang, S.; Zuo, J. L.; Zhou, H. C.; Choi, H. J.; Ke, Y.; Long, J. R.; You, X. Z. *Angew. Chem., Int. Ed.* **2004**, *43*, 5940. (p) Lee, I. S.; Long, J. R. *Dalton Trans.* **2004**, 3434. (q) Karadas, F.; Schelter, E. J.; Prosvirin, A. V.; Basca, J.; Dunbar, K. R. *Chem. Commun.* **2005**, 1414. (r) Beltran, L. M. C.; Long, J. R. *Acc. Chem. Res.* **2005**, *38*, 325. (s) Berlinguette, C. P.; Dunbar, K. R. *Chem. Commun.* **2005**, 19, 2451. (t) Berlinguette, C. P.; Dragulescu-Andrasi, A.; Sieber, A.; Gudiel, H. U.; Achim, C.; Dunbar, K. R. *J. Am. Chem. Soc.* **2005**, *127*, 6766. (u) Withers, J. R.; Ruschmann, C.; Bojang, P.; Parkin, S.; Holmes, S. M. *Inorg. Chem.* **2005**, *44*, 352. (v) Ni, Z. H.; Kou, H. Z.; Zhao, Y. H.; Zheng, L.; Wang, R. J.; Cui, A. L.; Sato, O. *Inorg. Chem.* **2005**, *44*, 2050.

* To whom correspondence should be addressed. E-mail: mallah@icmo.u-psud.fr.

[†] Laboratoire de Chimie Inorganique, ICMO, CNRS UMR 8613.

[‡] Laboratoire Louis Néel, CNRS.

- (1) (a) Mallah, T.; Auberger, C.; Verdager, M.; Veillet, P. *J. Chem. Soc., Chem. Commun.* **1995**, 61. (b) Scullier, A.; Mallah, T.; Verdager, M.; Nivorozhkin, A.; Tholence, J.-L.; Veillet, P. *New J. Chem.* **1996**, *20*, 1. (c) Langenberg, K. V.; Batten, S. R.; Berry, K. J.; Hockless, D. C. R.; Moubaraki, B.; Murray, K. S. *Inorg. Chem.* **1997**, *36*, 5006.

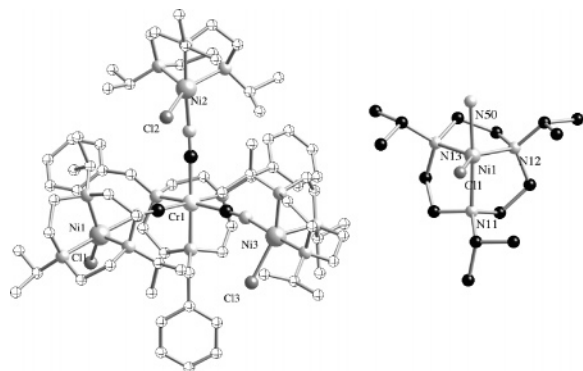


Figure 1. (left) View of the molecular structure of [BztacnCr(CNNi(iPrta)cn)Cl] $^{3+}$. (right) View of the structure of a Ni unit belonging to the tetranuclear complex. Hydrogen atoms were omitted for clarity.

few days by a slow diffusion of *tert*-butyl methyl ether into the mother solution.⁶

Compound **1** crystallizes in the monoclinic $P\bar{1}$ space group.⁷ The molecular structure of the tetranuclear complex (Figure 1, left) shows the central chromium atom linked to the Bztacn ligand and three cyanide groups in facial position

- (3) (a) Sokol, J. J.; Hee, A. G.; Long, J. R. *J. Am. Chem. Soc.* **2002**, *124*, 7656. (b) Berlinguette, C. P.; Vaughan, D.; Canada-Vilalta, C.; Galan-Mascaros, J. R.; Dunbar, K. R. *Angew. Chem., Int. Ed.* **2003**, *42*, 1523. (c) Palić, A. V.; Ostrovsky, S. M.; Klokischner, S. I.; Tsukerblat, B. S.; Berlinguette, C. P.; Dunbar, K. R.; Galan-Mascaros, J. R. *J. Am. Chem. Soc.* **2004**, *126*, 16860. (d) Wang, S.; Zuo, J. L.; Zhou, H. C.; Choi, H. J.; Ke, Y.; Long, J. R.; You, X. Z. *Angew. Chem., Int. Ed.* **2004**, *43*, 5940. (e) Choi, H. J.; Sokol, J. J.; Long, J. R. *Inorg. Chem.* **2004**, *43*, 1606. (f) Schelter, E. J.; Prosvirin, A. V.; Reiff, W. M.; Dunbar, K. R. *J. Am. Chem. Soc.* **2004**, *126*, 15004. (g) Choi, H. J.; Sokol, J. J.; Long, J. R. *J. Phys. Chem. Solids* **2004**, *65*, 839. (h) Miyasaka, H.; Takahashi, H.; Madanbashi, T.; Sugui, K.-I.; Clérac, R.; Nojiri, H. *Inorg. Chem.* **2005**, *44*, 5969.
- (4) The tacn-based ligands were prepared as already reported.⁵ The BztacnCr(CN) $_3$ was prepared from its bromide precursor⁵ BztacnCrBr $_3$ as described: 1.10 g (1.61×10^{-3} M) of BztacnCrBr $_3$ was dissolved in 10 mL of degassed DMSO and heated to 60 °C for 30 min under argon. A total of 5.81 g (1.2×10^{-1} M) of NaCN was added, and the reaction mixture was heated to 80 °C for 12 h. After cooling, the compound was precipitated as a pink-yellow solid upon the addition of 100 mL of water, filtered, washed with a small amount of cold water, and dried under vacuum. BztacnCr(CN) $_3$ is insoluble in water, methanol, ethanol, acetonitrile, acetone, THF, chloroform, and dichloromethane and very slightly soluble in DMSO and DMF. IR (KBr pellet): $\nu(\text{CN})$ 2125 cm^{-1} . Yield: 90%. $\chi_{\text{M}}T(295)$: 1.90 $\text{cm}^3 \text{mol}^{-1} \text{K}$. The iPrtaNiCl $_2$ complex was prepared as follows: 0.46 g (2×10^{-3} M) of NiCl $_2 \cdot 6\text{H}_2\text{O}$ was dissolved in 10 mL of methanol, 2 mL of trimethylorthoformate was added, and the solution was mixed with 30 mL of DME and 100 mL of THF. It was then heated under reflux for 10 min. Then 0.5 g (2×10^{-3} M) of iPrta was dissolved in 20 mL of THF, and this solution was added dropwise to the first solution. A green-yellowish precipitate appeared upon cooling of the solution. The precipitate was filtered, then dissolved in a minimum amount of chloroform, and precipitated by the addition of an excess of THF. The obtained solid was filtered, thoroughly washed with THF, and dried under vacuum. Anal. Calcd for C $_{15}\text{H}_{33}\text{Cl}_2\text{Ni}$ (%): C, 46.79; H, 8.64; N, 10.91; Cl, 18.42; Ni, 15.24. Found: C, 46.45; H, 8.77; N, 10.99; Cl, 18.39; Ni, 14.96. Yield: 67%. $\chi_{\text{M}}T(295)$: 1.15 $\text{cm}^3 \text{mol}^{-1} \text{K}$.
- (5) Haselhorst, G.; Stoetzel, S.; Strassburger, A.; Walz, W.; Wieghardt, K.; Nuber, B. *J. Chem. Soc., Dalton Trans.* **1993**, 83.
- (6) Anal. Calcd for **1** (%): C, 48.53; H, 8.36; N, 11.09; Cl, 11.31; Ni, 9.36; Cr, 2.76. Found: C, 48.41; H, 7.91; N, 11.09; Cl, 9.88; Ni, 9.24; Cr, 3.00. IR (KBr pellet): $\nu(\text{CN})$ 2131 cm^{-1} . Yield: 70%.
- (7) Crystal data for **1**: C $_{75}\text{H}_{168}\text{Cl}_6\text{CrNi}_{15}\text{O}_{18}$, fw = 2009.0, triclinic $P\bar{1}$, $T = 293 \pm 2$ K, $a = 17.2543(3)$ Å, $b = 17.8334(4)$ Å, $c = 19.3734(4)$ Å, $\alpha = 68.4360(10)^\circ$, $\beta = 66.7440(10)^\circ$, $\gamma = 82.9780(10)^\circ$, $V = 5091.73(18)$ Å 3 , $Z = 2$, $D_{\text{calc}} = 1.287$ g cm^{-3} , $F_{000} = 2082.00$, $\mu(\text{Mo K}\alpha) = 8.67$ cm^{-1} , final $R1 = 0.0574$ [$I > 4.00\sigma(I)$], $R = 0.0911$ (all data), $wR2 = 0.1545$ (all data), $\text{GOF} = 1.016$, $\rho_{\text{max}} = 0.832$ e Å $^{-3}$, $\rho_{\text{min}} = -0.674$ e Å $^{-3}$.

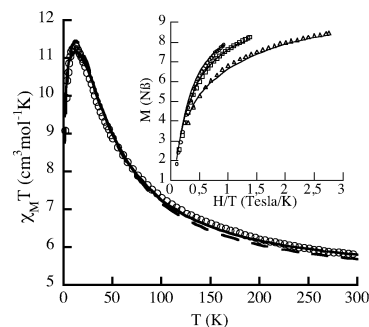


Figure 2. $\chi_{\text{M}}T = f(T)$ for **1**: (○) experimental data, (—) best fit including D , and (---) best fit including zJ (see text). Inset: $M = f(1/T)$, (○) $T = 6$ K, (□) $T = 4$ K, (Δ) $T = 2$ K, and (—) best fit.

bridging three Ni ions each capped by the iPrta ligand. The coordination sphere of the Ni atoms is pentacoordinated because only one chloride completes the coordination sphere (Figure 1, right). The geometries around the three crystallographically independent Ni atoms of the complex are similar and close to a distorted trigonal bipyramid.

The pseudotrigonal axis is along two nitrogen atoms: one from the bridging cyanide (N50) and the other (N11) belonging to the iPrta ligand; the N50–Ni1–N11 angle is almost linear and is equal to 176.8°. For the other two Ni units, this angle is mainly the same (176.6 and 176.7°). The base of the bipyramid is formed by the remaining nitrogen atoms of the organic ligand (N13 and N12) and the chloride atom. Because of the bite angle of the tacn-based ligand, the N12–Ni1–N13 angle is equal to 87.5° and the two N12–Ni1–Cl1 and N13–Ni1–Cl1 angles are equal to 144.0 and 128.5°, respectively. It is important to note that the pentacoordinated environment around the Ni atoms is probably due to the presence of the three *i*Pr groups on the capping ligand, which induces steric hindrance and prevents the coordination of the sixth ligand.

The N–C–Ni angles (where N–C is a cyanide ligand) are very close to linearity and range from 169 to 174°. Within the crystal, the molecules are quite far apart, with the shortest Ni–Ni distance belonging to two different molecules larger than 7.6 Å. However, the presence of water molecules creates a 2D H-bond network linking the clusters together within the crystal (Figure S1 in the Supporting Information).

The magnetic studies within the temperature range 300–2 K and for an applied field of 2000 Oe above 100 K and 100 Oe below (to avoid saturation effects) show that the $\chi_{\text{M}}T = f(T)$ curve increases upon cooling (Figure 2).

This is due to the presence of a ferromagnetic exchange coupling interaction between the central Cr(III) [$S = 3/2$; (d_{xy}) 1 (d_{xz}) 1 (d_{yz}) 1 electronic configuration] and the three Ni(II) [$S = 1$; (d_z) 1 ($d_{x^2-y^2}$) 1 configuration] ions as expected from the orthogonality of the magnetic orbitals.⁸ The $\chi_{\text{M}}T$ value at room temperature (5.8 $\text{cm}^3 \text{mol}^{-1} \text{K}$) is slightly higher than the expected one for uncoupled three Ni(II) ($S = 1$) and one Cr(III) ($S = 3/2$) metal ions (4.875 $\text{cm}^3 \text{mol}^{-1} \text{K}$ assuming the same g value equal to 2). The maximum value of $\chi_{\text{M}}T$ (11.3 $\text{cm}^3 \text{mol}^{-1} \text{K}$) at $T = 12$ K is slightly lower

- (8) Gadet, V.; Mallah, T.; Castro, I.; Verdager, M.; Veillet, P. *J. Am. Chem. Soc.* **1992**, *114*, 9213.

than that corresponding to $S = 9/2$ ($12.375 \text{ cm}^3 \text{ mol}^{-1} \text{ K}$ with an average g value of 2) arising from the ferromagnetic interaction. Below 12 K, $\chi_M T$ decreases. The lower value of $\chi_M T$ and the decrease at low temperature may be ascribed to zero-field splitting of the spin ground state and/or antiferromagnetic intermolecular interactions. The magnetic data can be modeled using the following Heisenberg spin Hamiltonian: $H = -J_{\text{Cr-Ni}}[S_{\text{Cr}} \cdot S_{\text{Ni1}} + S_{\text{Cr}} \cdot S_{\text{Ni2}} + S_{\text{Cr}} \cdot S_{\text{Ni3}}]$. The data were fitted for two cases: (i) considering only the zero-field splitting parameter D of the ground state $S = 9/2$ and (ii) considering only intermolecular interaction (zJ) within the near-field approximation. The two approaches give satisfactory results ($J_{\text{Cr-Ni}} = 20 \text{ cm}^{-1}$, $g = 2.07$, $|D| = 2.5 \text{ cm}^{-1}$ and $J_{\text{Cr-Ni}} = 20 \text{ cm}^{-1}$, $g = 2.03$, $zJ = -0.07 \text{ cm}^{-1}$). The quality of the fit is not improved by considering more than one J parameter because the J value is almost independent from the N–C–Ni angle for angles larger than 170° .⁹ The D value found does not reflect the real magnitude of the zero-field splitting of the ground state; it is overestimated because it reflects the decrease of $\chi_M T$ at low temperature, which may be due to antiferromagnetic intermolecular interactions as well. The best way to get a better idea of the D value is to fit the magnetization data at low temperature and a field higher than 0.5 T, where the intermolecular interactions are overcome. The magnetization data for **1** were measured at $T = 2, 4$, and 6 K in the field range 0.6–5.5 T (Figure 2, inset). The three curves are not superimposable, which is the signature of the presence of appreciable magnetic anisotropy within the compound. The magnetization value ($8.5 \mu_B$) at $H = 5.5 \text{ T}$ for the lowest temperature curve ($T = 2 \text{ K}$) is slightly lower than that for $9 \mu_B$ (expected value for a $S = 9/2$ ground state with $g = 2$). This is coherent with a $S = 9/2$ ground state experiencing some magnetic anisotropy. The energy difference between the ground $S = 9/2$ state and the first excited $S = 7/2$ spin state is around 30 cm^{-1} ($3J_{\text{Cr-Ni}}/2$). It is thus reasonable to assume that, even at $T = 6 \text{ K}$, only the ground state is populated. The $M = f(H/T)$ data were then fitted by calculating the magnetization versus field at the three temperatures for different orientations of the magnetic field. The best fit leads to $D = -0.54 \text{ cm}^{-1}$, $E/D = 0.29$, and $g = 2.00$ with an agreement factor $R = 5 \times 10^{-4}$. Magnetization studies give the magnitude of the anisotropy parameters; only detailed EPR studies may give accurate values. However, because a negative D value was obtained for complex **1**, we investigated its behavior at low temperature, where a blocking of the magnetization may be observed.

The magnetization studies were performed using an array of micro-SQUIDS on one single crystal oriented with its anisotropy axis parallel to the applied magnetic field. The magnetization versus field values were measured at $T = 40 \text{ mK}$ for different sweep rates of the magnetic field (only two sweep rates are shown below). The field was cycled between -1 and $+1 \text{ T}$ (Figure 3, left). A hysteresis is observed as a result of the slow relaxation of the magnetization. However,

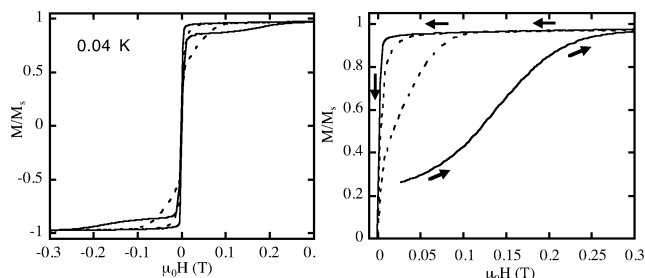


Figure 3. Micro-SQUID magnetization vs field studies at $T = 0.04 \text{ K}$ and between -1 and $+1 \text{ T}$ (left) and 0 and 1 T (right): (—) sweep rate 0.56 T s^{-1} ; (---) sweep rate 0.008 T s^{-1} . Only the data between -0.3 and $+0.3 \text{ T}$ are shown for clarity (see the Supporting Information).

the system shows a strong transition at $H = 0$ due to fast relaxation. To check whether the $H = 0$ transition is due to the tunneling of the magnetization, the sample was cooled from high temperature to 40 mK in zero field, getting a magnetization state with half of the spins up and the others down. We, then, ramped the field up to 1 T at different field sweep rates, observing a larger hysteresis effect than when the field was set at a negative field and cycled. This is a signature of the tunneling process at zero field because when starting at a negative field, all of the molecules are in the $M_S = S$ state and when the field approaches zero, most of them tunnel, leading to a strong transition at zero field (Figure 3, left). While when the field is set at zero (Figure 3, right), only half of the molecules are in the $M_S = S$ state, upon an increase in the field, half of them are blocked in the up state and they are not able to tunnel ($H > 0$), which leads to a larger hysteresis loop.¹⁰

For a half-integer spin state, the degeneracy of the Kramers doublets cannot be lifted by crystal field effects. So, no tunneling at zero field should be observed; however, very weak dipolar or exchange fields due to intermolecular interactions may do so. This is probably the case in the present compound because a 2D H-bond network linking the molecules together is indeed present.

In summary, metal complexes containing tacn derivatives allow one to build simple polynuclear complexes with well-defined ground states. Detailed EPR studies on **1** and on the mononuclear $\text{Ni}(\text{iPrtacn})\text{Cl}_2$ complex are underway in order to determine accurately the anisotropy parameters and the relationship between local anisotropy terms (D_{Ni} and E_{Ni}) and those related to the $S = 9/2$ ground state.

Acknowledgment. The authors thank the CNRS (Centre National de la Recherche Scientifique) and the European community for financial support (Contract MRTN-CT-2003-504880/RTN Network “QuEMolNa”).

Supporting Information Available: X-ray data for **1** in CIF format and Figures S1–S4. This material is available free of charge via the Internet at <http://pubs.acs.org>.

IC0514391

(9) Toma, L.; Toma, L. M.; Lescouëzec, R.; Armentano, D.; De Munno, G.; Andruh, M.; Cano, J.; Lloret, F.; Julve, M. *J. Chem. Soc., Dalton Trans.* **2005**, 1357.

(10) Such fast tunneling at zero field prevents the observation of dynamical magnetic behavior, so no ac signal was observed in the absence of a dc applied magnetic field.